A Compact F-band Filter Based on SiC Substrate-integrated Waveguides

Xiaopeng Wang, Mohammad Javid Asadi, Lei Li, Tianze Li, James C. M. Hwang
Cornell University
Ithaca, USA
xw569@cornell.edu

Fabian Thome, Peter Brückner, Dirk Schwantuschke
Fraunhofer Institute for Applied Solid State Physics IAF
Freiburg, Germany
Fabian.Thome@iaf.fraunhofer.de

***Abstract*—F-band substrate-integrated waveguides (SIWs) are designed, fabricated, and characterized on a SiC wafer, along with SIW-based filters, impedance standards, and transitions to grounded coplanar waveguides (GCPWs). The GCPW-SIW transitions not only facilitate wafer probing, but also double as resonators to form a 3-pole band-pass filter together with an SIW resonator. The resulted filter exhibits a 1.5-dB insertion loss at 115 GHz with a 34-dB return loss and a 19-GHz (16%) 3-dB bandwidth. The size of the filter is only 63% of previous filters comprising three SIW resonators. These results show the feasibility for monolithic integration of high-quality filters with high-efficiency antennas and amplifiers in a single-chip RF frontend above 110 GHz, which is particularly advantageous for 6G wireless communications and next-generation automobile radars.**

Keywords—cavity resonator, microwave filters, millimeter wave integrated circuits, semiconductor waveguides

I. Introduction

Similar to rectangular air-cavity waveguides, substrate-integrated waveguides (SIWs) have low loss, high power capacity, and minimum crosstalk, but are small, light, low-cost, and mass-producible [1], [2]. This is especially true for SIWs based on Si, GaAs and SiC that are commonly used in semiconductor processes. These SIWs are sufficiently small above 110 GHz, so that they can be monolithically integrated with other passive and active components to form a single-chip RF frontend [3], which is particularly advantageous for 6G wireless communications [4] and next-generation automobile radars [5].

SiC SIWs are attractive because high-power and high-efficiency GaN amplifiers are usually fabricated on SiC. SiC is high in dielectric constant, electrical resistivity, breakdown strength, mechanical toughness, and thermal conductivity, but low in loss tangent and thermal expansion coefficient [3]. Previously, for proof of principle, we used the custom process at Cornell University to design and fabricate a 3-pole filter comprising three SIW resonators, which exhibited a 1-dB insertion loss and a 25-dB return loss at 135 GHz [3]. In this paper, for monolithic integration feasibility, we used the foundry process for 100-nm GaN-on-SiC HEMT MMICs (GaN10) at Fraunhofer IAF [6] to design and fabricate another 3-pole filter comprising a SIW resonator and two SIW-GCPW transitions. The resulted filter has comparable performance but significantly smaller size as described in the following.

II. Design and Fabrication

The design of the present SiC SIW filter is aided by analytical modeling [7] and HFSS simulation. The filter is fabricated in a high-purity semi-insulating 4H c-axis SiC 100-mm wafer with a thickness of 75 ± 10 µm and a loss tangent as low as 3.7×10^{-5}. Consequently, the loss of the SIW is dominated by conductor loss instead of dielectric loss [8]. The fundamental TE_{10} mode propagating in the SIW is bound by a 3.5-µm-thick Au layer on the top and a 3-µm-thick Au layer on the bottom, as well as a row of through-substrate vias (TSVs) on each side. As shown in Fig. 1, the two rows of TSVs are separated by 520 µm center-to-center to cut off propagation below 100 GHz. The TSVs in each row have a 30-µm square cross section and are spaced 80-µm apart center-to-center. The TSVs are coated with 3-µm-thick Au. Typically, each TSV has a resistance < 0.1 Ω and an inductance of 24 pH.

To facilitate wafer probing, the SIW is transitioned [9], [10] to a grounded coplanar waveguide (GCPW) [11] at both the input and output. Each transition is 523-µm long, including a 33-µm GCPW section and a 490-µm tapered section. In the GCPW section, the center electrode is 20-µm wide with a 15-µm gap from the ground electrodes. In the tapered section, the center electrode is linearly widened to 120 µm while the gap is linearly widened to 120 µm. For the transition to double as a resonator, irises are formed by adding a 25-fF metal-insulator-metal (MIM) capacitor at the GCPW side and a rectangular gap at the SIW side. The MIM capacitor is 5-µm long and 20-µm wide with a silicon nitride insulator 0.3-µm thick. The rectangular gap is 80-µm long and 300-µm wide. To form a 3-pole filter, two transitions are used to sandwich a 380-µm-long SIW resonator in between, resulting in a total length of 1426 µm. If three SIW resonators and two transitions are used as in the previous design [3], the total length will be 2256 µm. Therefore, the present design is 37% smaller.

III. Results and Discussion

The fabricated SIW filter is probed from 10 MHz to 160 GHz using an Anritsu VectorStar ME7838G vector network analyzer (VNA) and two MPI TITAN 220-GHz coaxial probes with a 75-µm pitch. The input power of the VNA is fixed at −20 dBm. Using an MPI TCS-050-100-W impedance standard substrate and the line-reflect-reflect-match (LRRM) calibration method [12], the measured reflection and transmission coefficients, S_{11} and S_{21}, are rotated from the VNA to the probe tips.

Fig. 2 shows that measured S_{11} and S_{21} on five SIW filters agree with each other as well as the HFSS simulation. The average insertion loss and return loss are 1.53 dB and 21.7 dB, respectively, at the center frequency of 115 GHz. The 3-dB bandwidth is 18.7 GHz or 16%. Across the pass band, the insertion loss is flat within ±0.05 dB and the return loss is > 18 dB. The out-of-band rejection is higher than 30 dB and 20 dB below and above the pass band. Table I compares the performance characteristics of the present filter with that of

This work is supported in part by the Semiconductor Research Corporation and the US Defense Advanced Research Projects Agency

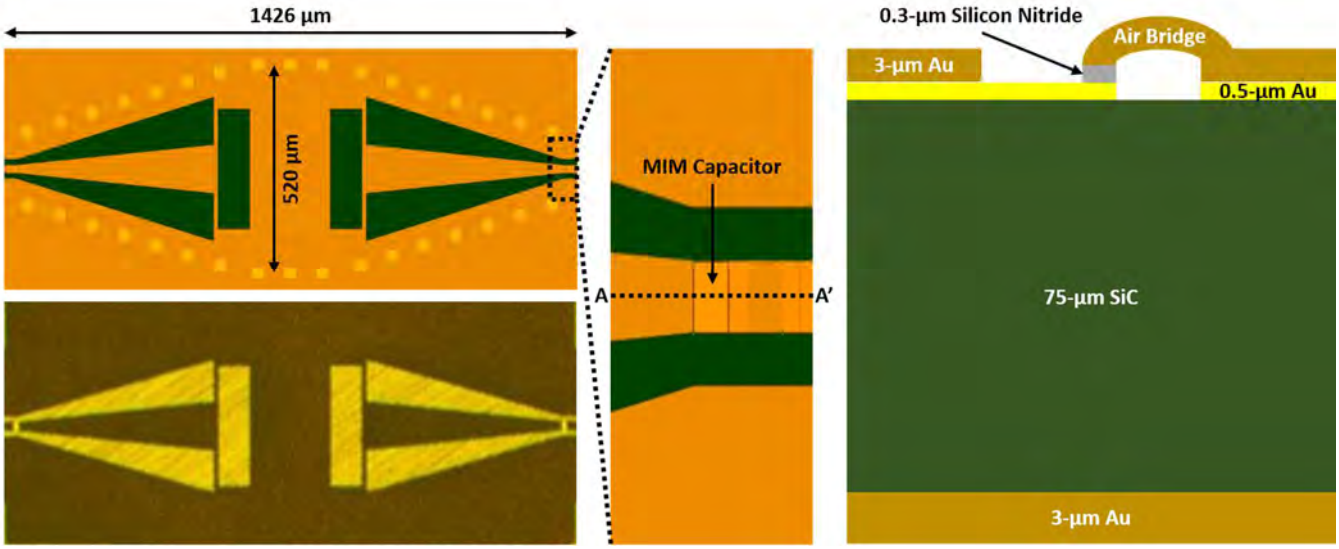

(a) (b) (c)

Fig. 1. (a) Layout (top) and chip micrograph (bottom) of a 3-pole F-band filter. (b) Detailed layout of an MIM capacitor. (c) A-A' cross-section of the MIM capacitor (not to scale).

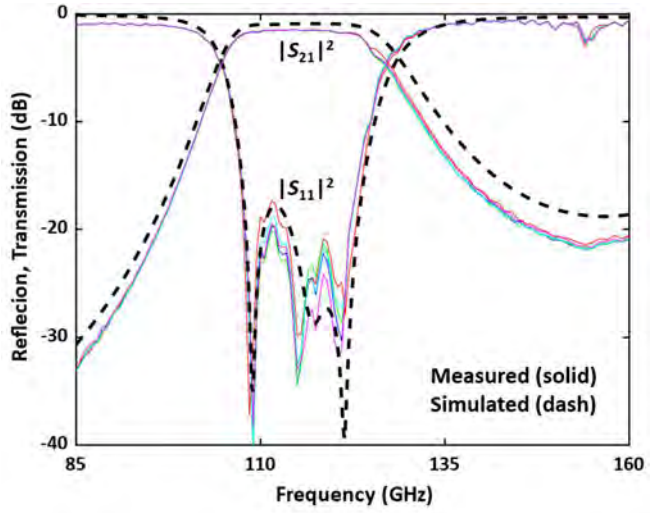

Fig. 2. Measured vs. simulated reflection and transmission coefficients. The measurement is performed on five 3-pole SiC SIW filters represented by curves of different colors. The simulation is performed by using a dielectric constant of 10.4.

the literature. Although it is difficult to compare filters of different bandwidths, it can be seen that the present filter is on par with the state of the art. It trades off a higher insertion loss for a wider bandwidth. In the future, the transition/resonator and its irises can be further optimized for a lower insertion loss. The out-of-band rejection can be improved by adding a transmission zero above the pass band.

The simulation uses a dielectric constant of 10.4 for SiC, which is very close to our experimentally extracted value of 10.3 [8]. Both are significantly higher than the commonly used value of 9.7 [16], which is actually for cubic SiC. In hexagonal SiC such as 6H SiC, [17] reports 9.66 for the ordinary permittivity and 10.03 for the extraordinary permittivity, both extrapolated from optical frequencies. The TE_{10} mode in an SIW made of c-axis SiC is governed by the extraordinary permittivity only [8] and directly measures the extraordinary permittivity of 4H SiC at millimeter-wave frequencies.

TABLE I
> 110 GHz FILERS BASED ON SUBSTRATE-INTEGRATED WAVEGUIDES

Year	Sub-strate	Freq. (GHz)	Insert. Loss (dB)	Return Loss (dB)	Band-width	Size (mm^2)	Ref.
2020	Si	279	9	20	1%	1.4×0.2	[13]
2020	Si	140, 280	3.9, 2.5	17, 11	10%	2.3×0.6	[14]
2017	SiC	183	~1	18	5%	0.9×0.6	[15]
2021	SiC	135	1.0	25	11%	2.3×0.6	[3]
2023	SiC	195.6	5.6	21.8	1.5%	1.2×1.2	[16]
2023	SiC	115	1.5	18	16%	1.4×0.6	This Work

IV. CONCLUSION

A compact F-band 3-pole filter is designed and fabricated by using a GaN-on-SiC HEMT MMIC foundry process to facilitate monolithic integration with other passive and active devices. The filter exhibits state-of-the-art performance but is significantly smaller. This shows the feasibility for monolithic integration of high-quality filters with high-efficiency antennas and amplifiers in a single-chip RF frontend above 110 GHz, which is particularly advantageous for 6G wireless communications and next-generation automobile radars.

ACKNOWLEDGMENT

The authors thank all colleagues in the Epitaxy and Technology Departments of Fraunhofer Institute for Applied Solid State Physics (Fraunhofer IAF), Freiburg, Germany, for their excellent contributions during epitaxial and wafer processing.

REFERENCES

[1] T. Yoneyama and S. Nishida, "Nonradiative dielectric waveguide for millimeter-wave integrated circuits," *IEEE Trans. Microw. Theory Techn.*, vol. 29, no. 11, pp. 1188–1192, Nov. 1981.

[2] D. Deslandes and K. Wu, "Substrate integrated transmission lines: Review and applications," *IEEE J. Microw.,* vol. 1, no. 1, pp. 345–363, Jan. 2021.

[3] M. J. Asadi, L. Li, K. Nomoto, Y. Tang, W. Zhao, P. Fay, D. Jena, H. G. Xing, and J. C. M. Hwang, "SiC Substrate-Integrated Waveguides for High-Power Monolithic Integrated Circuits Above 110 GHz," *2021*

IEEE MTT-S Int. Microw. Symp. (IMS), Atlanta, GA, USA, 2021, pp. 669–672.

[4] W. Hong, Z. H. Jiang, C. Yu, D. Hou, H. Wang, C. Guo, Y. Hu, L. Kuai, Y. Yu, Z. Jiang, Z. Chen, J. Chen, Z. Yu, J. Zhai, N. Zhang, L. Tian, F. Wu, G. Yang, Z.-C. Hao, and J. Y. Zhou, "The Role of Millimeter-Wave Technologies in 5G/6G Wireless Communications," *IEEE J. Microw.,* vol. 1, no. 1, pp. 101–122, Jan. 2021.

[5] F. A. Butt, J. N. Chattha, J. Ahmad, M. U. Zia, M. Rizwan, and I. H. Naqvi, "On the integration of enabling wireless technologies and sensor fusion for next-generation connected and autonomous vehicles," *IEEE Access,* vol. 10, pp. 14643–14668, Jan. 2022.

[6] F. Xu and K. Wu, "Guided-wave and leakage characteristics of substrate integrated waveguide," *IEEE Trans. Microw. Theory Techn.*, vol. 53, no. 1, pp. 66–73, Jan. 2005.

[7] F. Thome, P. Brückner, S. Leone and R. Quay, "A W/F-band low-noise power amplifier GaN MMIC with 3.5-5.5-dB noise figure and 22.8-24.3-dBm Pout," *2022 IEEE MTT-S Int. Microw. Symp. (IMS)*, Denver, CO, USA, 2022, pp. 603–606.

[8] L. Li, S. Reyes, M. J. Asadi, X. Wang, G. Fabi, E. Ozdemir, W. Wu, P. Fay, and J. C. M. Hwang, "Extraordinary permittivity characterization using 4H-SiC substrate-integrated waveguide resonators," *100th ARFTG Microw. Meas. Symp.,* Las Vegas, NV, USA, 2023, pp. 1–4.

[9] R. Kazemi, A. E. Fathy, S. Yang, and R. A. Sadeghzadeh, "Development of an ultra wide band GCPW to SIW transition," in *Proc. Radio Wireless Symp. (RWS)*, 2012, pp. 171–174.

[10] B. Krishnan and S. Raghavan, "A review on substrate integrated waveguide transitions," in *TEQIP III Sponsored Int. Conf. Microw. Integr. Circuits, Photonics Wireless Networks (IMICPW)*, 2019, pp. 424–428.

[11] Y. C. Shih and T. Itoh, "Analysis of conductor-backed coplanar waveguide," *Electron. Lett.*, vol. 18, no. 12, pp. 538–540, Jun. 1982.

[12] A. Davidson, K. Jones, and E. Strid, "LRM and LRRM calibrations with automatic determination of load inductance," in *ARFTG Conf. Dig.,* Monterrey, CA, Nov. 1990, pp. 57–63.

[13] A. Krivovitca, U. Shah, O. Glubokov, and J. Oberhammer, "Micromachined silicon-core substrate-integrated waveguides at 220-330 GHz," *IEEE Trans. Microw. Theory Techn.,* vol. 68, no. 12, pp. 5123–5131, Dec. 2020.

[14] G. Prigent, A. -L. Franc, M. Wietstruck, and M. Kaynak, "Substrate integrated waveguide bandpass filters implemented on silicon interposer for terahertz applications," *2020 IEEE MTT-S Int. Microw. Symp.,* 2020, pp. 595–598.

[15] Y. Li, L.-A. Yang, H. Zou, H.-S. Zhang, X.-H. Ma, and Y. Hao, "Substrate integrated waveguide structural transmission line and filter on silicon carbide substrate," *IEEE Electron Device Lett.,* vol. 38, no. 9, pp. 1290–1293, Sep. 2017.

[16] Y. Liu, L. -A. Yang, Y. Li, S. Liu, Y. Chen, X. Zhang, X. Ma, and Y. Hao, "Terahertz monolithic integrated narrow-band filter based on the silicon carbide substrate," *Semicond. Sci. Technol.*, vol. 38, no. 1, pp. 035002, Jan. 2023.

[17] L. Patrick and W. J. Choyke, "Static dielectric constant of SiC," Phys. Rev. B, vol. 2, no. 6, pp. 2255–2256, Sep. 1970.